Int. J. Multiphase Flow Vol. 6, pp. 203–215
Pergamon/Elsevier, 1980. Printed in Great Britain

LONGITUDINAL FLOW CHARACTERISTICS OF VERTICALLY FALLING LIQUID FILMS WITHOUT CONCURRENT GAS FLOW

HEISHICHIRO TAKAHAMA
Department of Mechanical Engineering, Faculty of Engineering, Nagoya University, Furo-cho, Chikusa-ku, Nagoya 464, Japan

and

SEIZO KATO
Department of Mechanical Engineering, School of Engineering, Mie University, Kamihama-cho, Tsu 514, Japan

(*Received* 27 *April* 1979; *in revised form* 1 *November* 1979)

Abstract—Flow characteristics of liquid films vertically falling along the outer wall of a circular tube without concurrent gas flow are experimentally studied, and attention is given to the longitudinally developing liquid film flow in the flow direction. Flow measurements are carried out by the methods of needle contact and electric capacity, and the obtained data are statistically processed.

There exists a definite difference in flow characteristics such as wave motion patterns, film thicknesses, critical Reynolds number, and so on, depending strongly on the longitudinal distance in the flow direction as well as the liquid film Reynolds number. Measured probability distributions of interfacial waves can be well expressed by the functions of probability distribution statistically well-known as normal, logarithmic normal and gamma distributions. In terms of these functions, interfacial wave patterns are definitely classified over the whole experimental flow regime. As a rule, interfacial wave motion proceeds vigorously with increases of the longitudinal distance and Reynolds number; however, there exists a flow condition that wave fluctuation never grows up but declines regardless of an increase of Reynolds number.

1. INTRODUCTION

Vertically falling liquid film flow along a solid surface is widely encountered and has various industrial applications, especially in chemical engineering. Extensive research on falling liquid films, therefore, has been performed as a subject of study independently of annular gas/liquid two phase flow (e.g. Levich 1962, Fulford 1964, Dukler 1972). Knowledge of microscopic flow characteristics including interfacial wave phenomena, however, is not sufficient to provide a quantitative prediction of transport rates like heat and mass transfer in liquid films.

According to observations of vertically falling liquid films by one of the present authors (Takahama *et al.* 1974), virtually all of the interface of liquid film are always covered with unsteady and irregular waves whose behaviour depends on not only liquid and gaseous Reynolds numbers but also the longitudinal distance in the flow direction. This fact indicates that theoretical analyses under the assumption of periodic solutions and theories for single phase are inapplicable, and that the application of experimental results obtained at a fixed longitudinal distance to the whole flow field is altogether incorrect. Consequently, it is practically important to determine the dependence of flow characteristics on the longitudinal distance, and to relate it with quantitative transport rates in the flow system. No effective ways are presently available to describe generally unsteady wavy films, but a recent statistical method seems reasonable and in fact provides remarkably interesting information (Telles & Dukler 1970, Chu & Dukler 1974, 1975, Sekoguchi *et al.* 1973, 1977).

This paper is concerned with experimental analysis of the longitudinally developing process of vertically falling liquid films, in order to provide fundamental data to correlate with heat and mass transfer in liquid films. We deal here with water films falling along the outer wall of a vertical circular tube without concurrent gas flow. The data obtained by flow measurements are statistically processed and discussed mainly from the standpoint of longitudinal flow behavior along the film flow. No measurements on internal structure such as velocity distribution and

shearing stresses are carried out in this study. Taking account of the poor reliability as to the accuracy of such measurements thus far, however, we believe that the present results, obtained by accurate measurements, form a reliable foundation for the hydrodynamical analysis of liquid films.

2. EXPERIMENTAL APPARATUS AND MEASUREMENTS

The experimental apparatus is shown schematically in figure 1. The test channel is a brass cylinder finished accurately to 44.92 ± 0.02 mm in diameter and 2 m long, and it is set up vertically. Water fed through a slit-type distributor flows down vertically as a falling liquid film along the outer surface of the cylinder. A 40 μ porous sinter section is occasionaly used in the case of a small rate of flow. Liquid temperature is always measured by thermocouples at the inlet and exit of the test section, and is maintained at 17.0 ± 0.3°C by submergible heaters.

Measurements of wavy liquid films are carried out by the methods of needle contact and electric capacity. The needle used here is a quenched sewing needle having 35 μ radius at the tip, with attention paid to the abrasion occurring on the tip at zero point adjustment. The probe used in the electric capacity method is a copper cylinder of 2 mm diameter, and is kept away so as not to touch the wavy films. Because of a nonlinear relation between film thickness and output in the capacity method, the calibration is made at every run. In connection with the probability distribution of wavy films, the agreement between the above two methods is obtained at the flow condition of the film Reynolds number $Re = \Gamma/\nu > 300$ in the study, where Γ is the volumetric flow rate of liquid per wetted perimeter and ν is the kinematic viscosity of liquid.

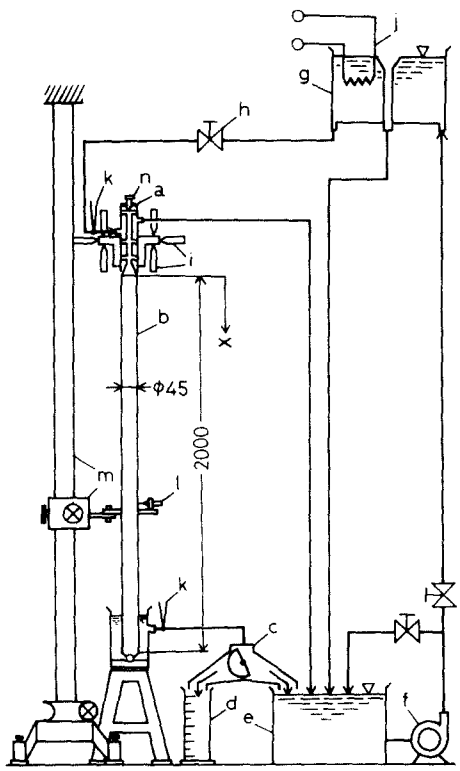

Figure 1. Schematic diagram of the experimental layout. (a) distributor, (b) test channel, (c) switching device of flow direction, (d) measuring tank for flow rate, (e) lower cistern, (f) water pump, (g) upper cistern, (h) regulating valve, (i) verticality adjusting device, (j) heater, (k) thermocouple, (l) probe for film measurement, (m) probe positioning device, (n) micrometer for flow rate adjustment.

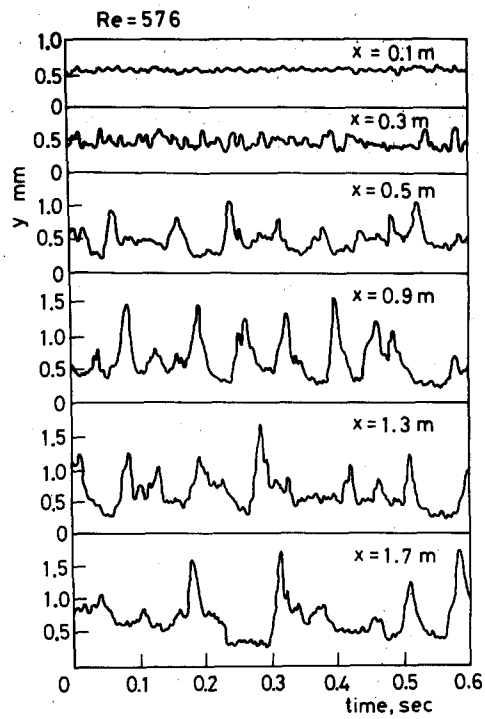

Figure 2. Longitudinal developing process of interfacial wave form.

3. OBSERVATION OF INTERFACIAL WAVES

Interfacial waves of liquid films are observed by the capacity method in order to qualitatively grasp the longitudinal flow characteristics. A typical result for $Re = 576$ is shown in figure 2, in which x indicates the longitudinal distance in the flow direction from the test channel entrance. At the entrance region of the longitudinal distance of $x = 100$ mm, waves having a small amplitude of less than 0.1 mm and a high frequency of nearly 100 Hz are observed, which are regarded to be a so-called mirror surface by visual observation. At $x = 300$ mm, ripple type waves of about 0.3 mm in amplitude and about 50 Hz in frequency are observed. Then, such waves develop into appreciably isolated large waves at $x = 500 \sim 900$ mm. The respective large waves fall two-dimensionally to the trailing edge of the test section; namely, they descend without any change in shape. The frequency decreases to $10 \sim 20$ Hz and the maximum height reaches about 1.5 mm. These type waves surely have the structure of a two-wave system which consists of a substrate and a large waves (Telles & Dukler 1970, Chu & Dukler 1974, 1975, Sekoguchi *et al.* 1973). It is evident that wave motion is affected not only in terms of Reynolds number but also longitudinal distance.

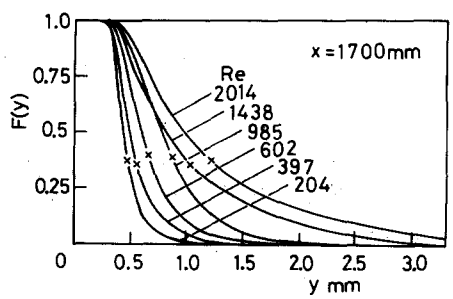

Figure 3. Typical results of measured probability distributions. Cross symbol designates mean film thickness.

4. DISCUSSION OF FLOW CHARACTERISTICS USING MEAN FILM THICKNESS

4.1 *Mean film thickness*

The mean film thickness in this paper is evaluated from the following procedure. First, the probability distribution of the liquid film, $F(y)$, as shown in figure 3, which indicates the ratio of the time that the needle at a normal distance from the wall surface, y, is touching the liquid film to the total measuring time, is obtained by the needle contact method at eight positions along the circumference of the circular tube. Then, the respective mean film thicknesses are evaluated from graphical integration of their respective curves. After the eight mean film thicknesses are checked for an allowable deviation of less than 2%, their arithmetically averaged value is defined as the mean film thickness, $\bar{\delta}$.

The foot of the measured probability distribution as shown in figure 3 extends with an increase of Re; however, the value of $F(y)$ corresponding to $\bar{\delta}$ is roughly constant and lies between $0.35 \sim 0.41$ (its mean value is 0.38). Figure 4 shows the dependence of mean film thickness on longitudinal distance. At a small Reynolds number of $Re = 200$, $\bar{\delta}$ at $x = 100$ mm decreases only 3 percent even at $x = 1700$ mm. On the other hand, at a large Reynolds number of $Re = 997$, $\bar{\delta}$ increases rapidly at the entrance region of $x < 500$ mm, but at a greater longitudinal distance $\bar{\delta}$ becomes approximately constant. At the intermediate Reynolds number between 200 and 997, however, the behavior of mean film thickness is rather peculiar, for with an increase of x, $\bar{\delta}$ increases at the entrance region to a maximum value, decreases to a minimum level and then increases again. The flow at the intermediate Reynolds number is rather unstable and this instability occasionally tends to scatter the experimental values. Such peculiar behavior seems to derive from a substantial change in the longitudinal flow characteristics of liquid films, which will be discussed in the next section.

4.2 *Longitudinal change of critical Reynolds number*

Transition from laminar to turbulent flow may be considered to cause the peculiar behavior mentioned above. Therefore, the longitudinal change of the critical Reynolds number is estimated here.

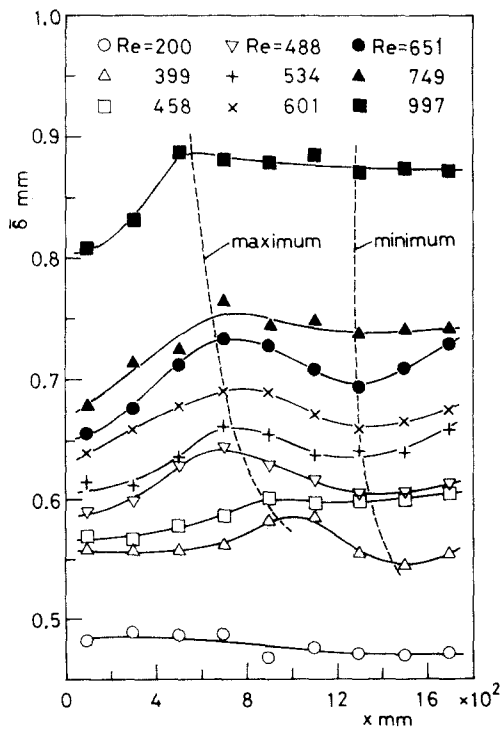

Figure 4. Longitudinal distributions of mean film thickness.

Variation of mean film thickness against Reynolds number is plotted for longitudinal distance as a parameter in figure 5, in which Brauer's experimental results obtained at film temperature of 27.5°C are included. Theories for laminar and tubrulent flow are also compared. We chose here as a theoretical standard Nusselt's theory of laminar flow:

$$\bar{\delta} = (3\nu^2 Re/g)^{1/3}, \qquad [1]$$

where g is the acceleration of gravity. The theory is designated by a broken line in the figure. As for turbulent flow, the mean film thickness is well expressed by Brauer's empirical formula:

$$\bar{\delta} = 0.302(3\nu^2/g)^{1/3} Re^{8/15}, \qquad [2]$$

which is shown by a single-dot-dash-line. A theoretical expression derived from Karman's universal velocity distribution (Dukler & Bergelin 1952) is given by the following form:

$$(3.0 + 2.5 \ln \bar{\delta}^+)\bar{\delta}^+ = Re + 64, \qquad [3]$$

where $\bar{\delta}^+ = u^*\bar{\delta}/\nu$ and u^* is the friction velocity, the latter being evaluated from a force balance of wall friction and gravity force as follows:

$$u^* = \sqrt{(g\bar{\delta})}, \qquad [4]$$

and is also yielded from the Navier–Stokes equation as (Yoshioka *et al.* 1971)

$$u^* = \{g\nu/(27.5/30.0\bar{\delta}^+) - 2.5/\bar{\delta}^+\}^{1/3}. \qquad [5]$$

Comparison of the experimental results with the above expressions shows that at the flow regime of $Re < 400$ the experimental results are parallel to those of Nusselt's theory and are

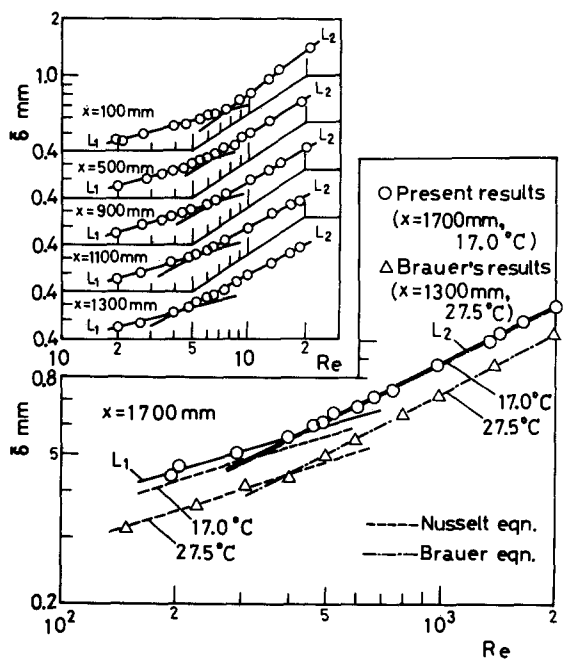

Figure 5. Dependence of mean film thickness of Reynolds number and definition of critical Reynolds number.

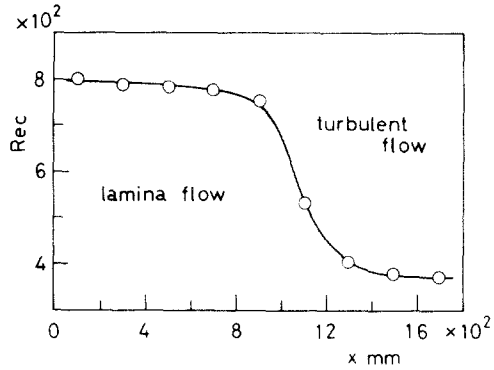

Figure 6. Longitudinal change of critical Reynolds number.

only 5 per cent larger than those of the theory. This fact may imply that the liquid films are characterized by a kind of laminar flow. At the region of $Re > 400$, the experimental results tend to well coincide with Brauer's equation[2] for turbulent flow (presentation of the theory[3] is omitted in the figure because the theoretical and Brauer's values almost agree in the fully developed turbulent flow regime). Therefore, the flow property is transformed into the regime of turbulent flow. Thus, all of the curves obtained at different positions of x seem to be approximately replaced by two linear solid lines of L_1 for a kind of laminar flow and L_2 for turbulent flow as shown in the figure.

The critical Reynolds number, Rec, is defined here as the intersection of the two lines of L_1 and L_2, and the dependence of Rec on x is shown in figure 6. Rec at $x < 800$ mm remains nearly constant at $750 \sim 800$, then at $x = 900 \sim 1300$ mm it rapidly drops to about 400, and finally once more maintains a constant value of 370. It is worth noting that the range where the critical Reynolds number depends on the longitudinal distance corresponds well to the range where the peculiar dependence of the mean film thickness on the longitudinal distance occurs as mentioned in section 4.1. Therefore, it may be considered that the peculiarity mainly results from instability of this transition process in the longitudinal flow direction.

Since the critical Reynolds number is a function of the longitudinal distance, care should be taken in fixing a position for film measurements, with attention paid to the fact that the critical Reynolds number maintains a constant value only at $x > 1300$ mm.

The theory of turbulent flow, i.e.[3], can express the experimental results more accurately with the aid of[5] than of[4]. Evaluation of the critical Reynolds number from[5] leads to $Rec = 368$ and from[4] $Rec = 270$, the former agreeing very closely with the present experimental result.

The mean film thickness in the turbulent flow regime is approximately given by the following empirical formula:

$$\bar{\delta} = 0.473(\nu^2/g)^{1/3} Re^{0.526}. \qquad [6]$$

5. WAVE PROPERTIES

5.1 *Maximum and minimum film thicknesses*

Figure 7 shows the longitudinal distributions of the maximum film thickness, δ_{max}, and the minimum film thickness, δ_{min}, in which δ_{max} and δ_{min} are defined as the values of y corresponding to $F(y) = 1$ and $F(y) = 0$, respectively. We find that δ_{max} increases linearly with an increase of x except in the entrance region where it increases more rapidly. Another peculiar phenomenon is that the magnitude of δ_{max} at $Re = 601$ and 749 becomes reverse at $x > 1000$ mm, and this is later considered in section 6.3. On the other hand, δ_{min} decreases at the entrance region; however, at a greater longitudinal distance δ_{min} becomes almost constant independently of Re and x.

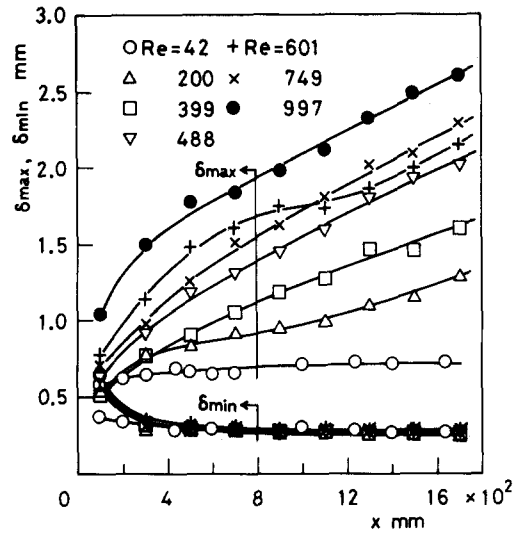

Figure 7. Longitudinal distributions of maximum and minimum film thicknesses.

The longitudinal distribution of the dimensionless maximum wave height, $(\delta_{max} - \delta_{min})/\bar{\delta}$, shows qualitatively a similar tendency to that of δ_{max} as shown in figure 7. The wave height is nearly the same order of $\bar{\delta}$ even at the entrance region of $x = 200 \sim 300$ mm, and increases linearly with an increase of x attaining several times the mean film thickness (about ten times the minimum film thickness) at the distance of $x = 1700$ mm. Therefore, it is found that the two-dimensional large wave carries a significant portion of liquid film, so this type wave contributes substantially to the transport mechanism in liquid films.

5.2 *Frequency and separation distance of large waves*

The wave frequency, f, and the separation distance, L, of large waves were measured by the capacity method, and the typical results are shown in figure 8. As liquid film flows down under the condition of a constant Reynolds number, the frequency decreases to the order of 10 Hz and the separation distance increases to about 15 cm. On the other hand, it is found that both f and L increase with an increase of Re; however, the increasing rates of f and L against Re asymptotically decrease to the respective constant values of $f \approx 10$ Hz and $L \approx 20$ cm at $x = 1500$ mm.

Figure 9 shows the longitudinal change of frequency analysis measured at $Re = 513$, in which the ordinate indicates the ratio of output of band-pass to that of all-pass, i.e. output ratio. At the entrance region of $x < 300$ mm, waves having height frequency of the order of

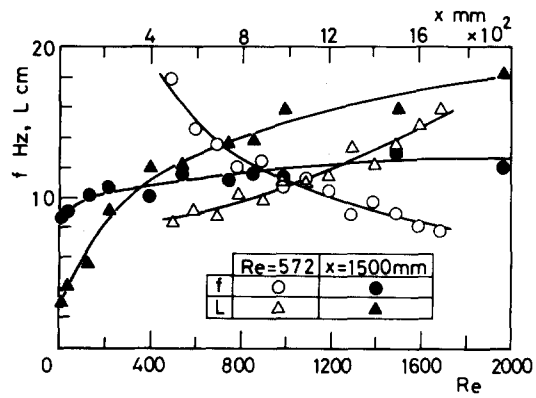

Figure 8. Frequency and separation distance of large waves.

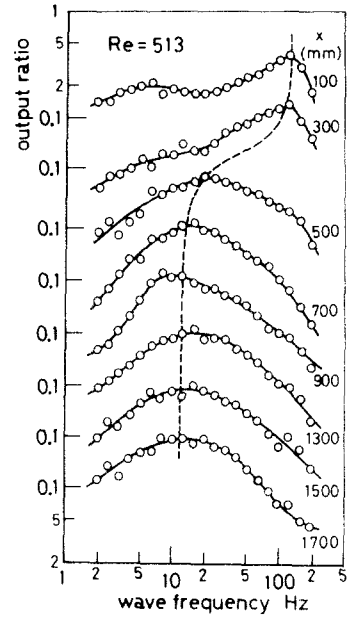

Figure 9. Typical results of frequency analysis of interfacial waves. Broken line indicates longitudinal change of frequency corresponding to peak value of output ratio.

100 Hz are considerably dominant and the peak value of the output ratio is obtained at nearly 100 Hz. The frequency corresponding to the peak value decreases rapidly at $x = 300 \sim 700$ mm to about 10 Hz, and it remains constant over greater longitudinal distance, as shown by a broken line. At $x > 500$ mm, large waves with the frequency of the order of 10 Hz tend to prevail. Thus, we can find that the number of large waves is rather few in the whole test section.

5.3 *Wave celerity*

The wave celerity of the large waves, c, is estimated from a time difference while a steady large wave passes between two electrodes. The result is shown in figure 10, in which $\bar{v} = \Gamma/\bar{\delta}$ is the mean velocity of liquid films. The wave celerity considerably decreases at the entrance region of $x < 600$ mm, and then approaches a constant value over the greater longitudinal distance. The mean velocity is also kept to an almost constant value at that distance, so the

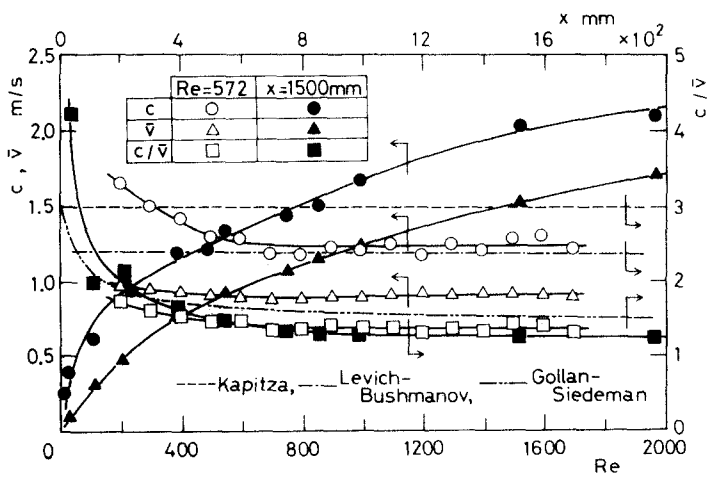

Figure 10. Dependence of wave celerity, mean velocity and their ratio on Reynolds number and on longitudinal distance.

ratio of $c/\bar{v}$ becomes a constant value of about 1.3 independently of Re and x. The theories derived by Kapitza (1948), Levich & Bushmanov (1962), and Gollan & Siedeman (1969) are unable to be applied to practical liquid films covered with large waves, because large waves have neither periodic nor linear nature.

5.4 *Surface area increase due to interfacial waves*

In order to examine the effect of the surface area increase due to the interfacial waves on the transport rates, the surface area increment relative to the smooth surface without waves, β, is estimated from the wave form (figure 2) with the aid of a rotary length measuring device. The result is presented in figure 11, in which $(\beta - 1)$ is the net increment of wavy surface area. It is evident that $(\beta - 1)$ increases as Re and x increase; however, the value is less than 0.03 per cent. Hence, it may be concluded that promotion of heat and mass transfer in liquid films is not due to an increase of the interfacial surface area but to the disturbance effect by the large wave motion. motion.

6. STATISTICAL DISCUSSION OF WAVE MOTION

6.1 *Wave amplitude*

Interfacial wave motion is essentially random but has a stochastic property as shown in figure 3. Hence, the probability distribution, $F(y)$, obtained by the experiment can be connected with the probability density function, $f(y)$, as

$$dF(y)/dy = f(y), \qquad [7]$$

and the first order moment is given by

$$\int_0^\infty yf(y)dy = \bar{\delta}. \qquad [8]$$

This moment is equal to the mean film thickness, $\bar{\delta}$. The second order moment about $\bar{\delta}$ leads to the following expression:

$$\int_0^\infty (y - \bar{\delta})^2 f(y)dy = s^2, \qquad [9]$$

where s^2 is the variance and s the standard deviation. Figure 12 shows a developing process of the variance evaluated by graphic integration of [9] in the longitudinal flow direction. Under the flow condition of $Re < 1000$, s^2 is still small at the entrance region of $x < 500$ mm; thus, an appreciably large wave motion does not occur as yet. As x increases to a greater longitudinal distance, however, s^2 rapidly increases, implying that the large waves with larger wave height

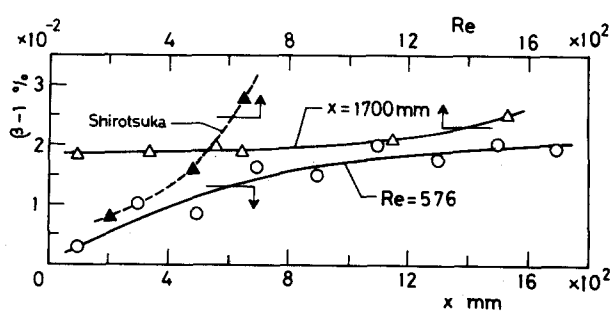

Figure 11. Net increment of surface area due to interfacial waves relative to smooth surface without waves.

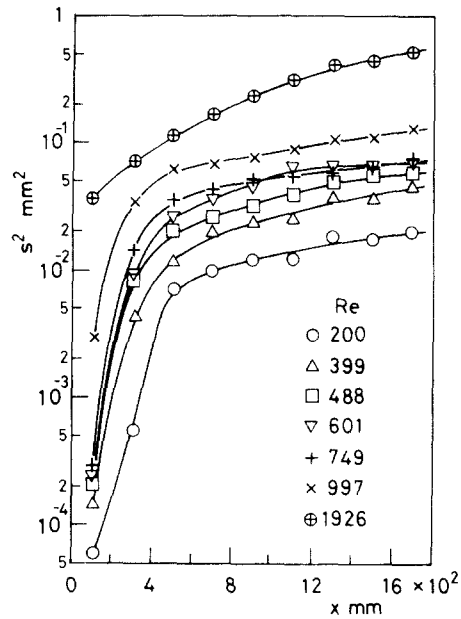

Figure 12. Longitudinal distributions of variance of interfacial wave motion.

prevail. In the case of $Re > 1000$, even at $x = 100$ mm an appreciable fluctuation due to the large waves occurs. However, the variance has a limiting value depending on Re, i.e. there is a limit for amplification of the wave height. This limiting value expressed in terms of $s/\bar{\delta}$ is $0.3 \sim 0.7$. This fact suggests that the large lumps of liquid films are carried by the large waves.

6.2 *Classification of wave property*

It is practically useful to specify the measured probability distribution by statistically well-known functions of probability distribution. At first, the measured probability distribution is plotted on the normal probability distribution graph, and the region with waves having a normal distribution property is distinguished. Then, the region were the logarithmic normal probability distribution holds is also established using logarithmic normal probability distribution graph. For the region where both distribution functions do not apply, it is found that the gamma function well expresses the measured probability distribution. Thus, the classification in terms of the above three distribution functions is shown in figure 13. The wave

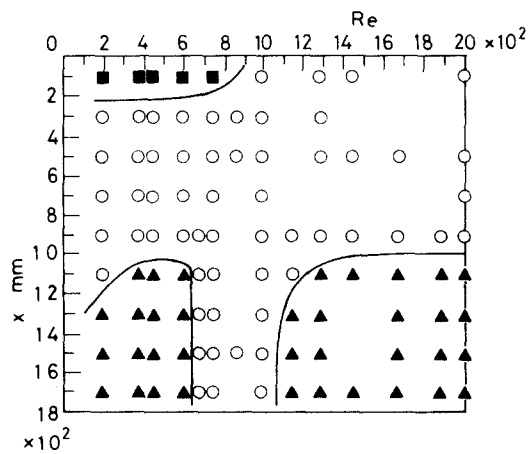

Figure 13. Classification of wave characteristics by means of probability distribution functions. Square ■, circle ○, and triangle ▲ designate normal, logarithmic normal and gamma distribution functions, respectively.

property of vertically falling liquid films is definitely classified into the three domains. The normal distribution region is confined only to the entrance region of $x < 200$ mm as well as the small Reynolds number of $Re < 900$. Therefore, the flow condition under which the assumption of the periodic solution is reasonable seems extremely limited in the practical order. In the actually used flow condition, the interfacial wave motion has the properties of the logarithmic normal and gamma distributions. Further, it is interesting that there is a domain of the logarithmic normal distribution in which both boundaries at $x > 1000$ mm are surrounded by the gamma distributions.

6.3 *Correlation with maximum film thickness*

The variance is closely associated with the maximum film thickness, because the minimum film thickness hardly changes. The correlation between s^2 and δ_{max} is shown in figure 14, which includes not only s^2 and δ_{max} at $x = 1300$ mm but also s^2 at $x = 500$, 900 and 1700 mm for reference. Ishigai *et al.* (1972) provide an alternative classification of flow patterns in vertically falling liquid films by means of a maximum film thickness of $x = 1450$ mm. The symbol IV, V, VI on the curve of δ_{max} correspond to the flow regions classified by them. The region of IV is the transition one from steady wave motion to turbulent flow, and the turbulent flow regions are denoted by V and VI with no distinction between them.

The present results of δ_{max} as well as δ_1 (1 per cent film thickness) at $x = 1300$ mm definitely show a remarkable finding, namely, both thicknesses display almost no increase with an increase of Re over the range of $Re = 400 \sim 800$. In this V region, s^2 at $x = 1300$ mm also remains constant. And this region approximately corresponds to the domain of the logarithmic normal distribution in which both boundaries are surrounded by the gamma distributions as indicated in the figure. This striking behavior surely holds at $x = 1700$ mm as well. In general, wherever the logarithmic normal distribution surrounded by the gamma distributions on the both sides prevails at $x > 1000$ mm and $Re = 400 \sim 800$, such behavior is certainly maintained. Consequently, in this flow region the interfacial wave fluctuation never grows up but once declines regardless of an increase of Reynolds number, and this characteristic implies that there exists a prior stage of the fully developed turbulent flow regime.

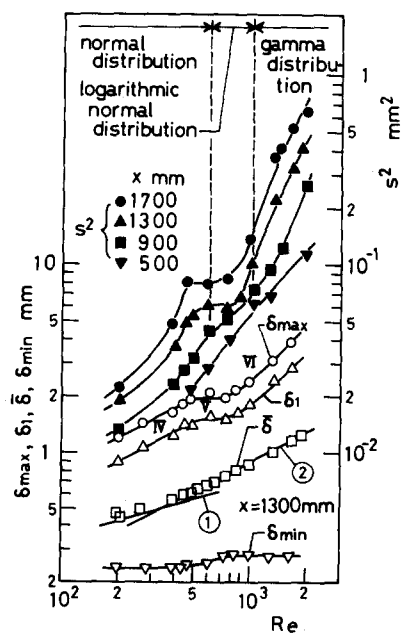

Figure 14. Correlation of statistical characteristics of interfacial waves with maximum film thickness. Line ① and line ② are Nusselt's theory (1) for laminar flow and empirical equation (6) for turbulent flow.

The peculiar phenomenon in which the maximum film thickness at $Re = 601$ and 749 becomes reverse at $x > 1000$ mm as described in section 5.1 can be attributed to the fact that since the flow condition at $Re = 749$ enters this V region, the maximum film thickness becomes smaller than that for $Re = 601$. In fact, the corresponding variance shows a tendency similar to that of the maximum film thickness, as shown in figure 12.

At a longitudinal distance of $x < 900$ mm, on the contrary, the peculiarity mentioned never occurs, so there is a difference in flow development depending on the longitudinal distance in the flow direction of the falling liquid films.

7. CONCLUSIONS

Flow characteristics of longitudinally developing liquid films in the flow direction without concurrent gas flow have been experimentally studied, and the following conclusions could be derived from the results:

(1) The critical Reynolds number based on the mean film thickness depends on the longitudinal distance, for Rec remains constant at $750 \sim 800$ at $x < 900$ mm, but decreases remarkably at $x = 900 \sim 1300$ mm, approaching 380 at $x > 1300$ mm.

(2) The wave amplitude increases with increases of Re and x, but its maximum magnitude has a limiting value of $s/\bar{\delta} = 0.2 \sim 0.5$ in the experimental range. The number of large waves on the test section is rather few, judging from the values of the wave frequency, the separation distance, and the wave celerity. Moreover, the surface area increases due to the interfacial waves is neglegible small.

(3) The measured probability distribution of liquid films can be well expressed by the well-known probability distribution functions of the normal, the logarithmic normal, and the gamma distributions. By these functions the wave characteristic can be classified definitely over the whole test conditions.

(4) As a rule, the interfacial wave motion proceeds vigorously with increases of the longitudinal distance and Reynolds number. However, in the region of $x > 1000$ mm and $Re = 400 \sim 800$, the wave fluctuation never grows up but declines regardless of an increase of Reynolds number.

Acknowledgement—The authors wish to acknowledge the great assistance of Mr. T. Kiuchi in this study.

REFERENCES

BRAUER, H. 1956 Strömung and Wärmeübergang bei Reiselfilmen. *VDI-Forschungsheft* 457.

CHU, K. J. & DUKLER, A. E. 1974 Statistical characteristics of thin, wavy films—II. Studies of the substrate and its wave structure. *AIChE J.* **20**, 695–706.

CHU, K. J. & DUKLER, A. E. 1975 Statistical characteristics of thin, wavy films—III. Structure of the large waves and their resistance to gas flow. *AIChE J.* **21**, 583–593.

DUKLER, A. E. & BERGELIN, O. P. 1952 Characteristics of flow in falling liquid films. *Chem. Engng Prog.* **48**, 557–563.

DUKLER, A. E. 1972 Characterization, effects and modeling of the wavy gas-liquid interface. *Prog. Heat and Mass Trans.* **6**, 207–234.

FULFORD, G. D. 1964 The flow of liquids in thin films. *Advan. Chem Engng* **5**, 151–236.

GOLLAN, A. & SIEDEMAN, S. 1969 On the wave characteristics of falling films. *AIChE J.* **15**, 301–303.

ISHIGAI, S., NAKANISHI, S., KOIZUMI, T. & OYABU, Z. 1972 Hydrodynamics and heat transfer of vertical falling liquid films—1. Classification of flow regimes. *Bull. of Japan Soc. Mech. Engrs* **15**, 594–602.

KAPITZA, P. L. 1964 Wave flow of thin layers of a viscous fluid. In *Collected Papers of P. L. Kapitza*, Vol. 2, pp. 662–713. Macmillan, New York.

LEVICH, V. G. 1962 *Physicochemical Hydrodynamics.* Prentice Hall, New Jersey.

SEKOGUCHI, K., NISHIKAWA, K., NAKAZATOMI, M., NISHI, H. & KANEUJI, A. 1973 Liquid film flow phenomena in upwards two-phase annular flow. *Trans Japan Soc. Mech. Engrs* **39**, 313–323.

SEKOGUCHI, K., HORI, K., NAKAZATOMI, M., NAKANO, K. & NISHIKAWA, K. 1977 On ripple of annular two-phase flow—1. Statistic characteristic of ripples. *Bull. Japan Soc. Mech. Engrs* **20**, 844–851.

SHIROTSUKA, T., HONDA, N. & OHATA, Y. 1957 Wave motion on the falling liquid film in a wetted-wall column of flat plate. *Chem. Engng (Japan)* **21**, 702–707.

TAKAHAMA, H., FUJITA, H., KODAMA, T., KURIBAYASHI, M. & AISO, T. 1974 Heat and mass transfer in countercurrent flow of air and water film in a rectangular vertical duct. *Bull. Japan Soc. Mech. Engrs* **17**, 928–935.

TELLES, A. S. & DUKLER, A. E. 1970 Statistical characteristics of thin, vertical, wavy, liquid films. *Ind. Engng Chem. Fundam.* **9**, 412–421.

YOSHIOKA, K., YOSHIMATSU, M. & HASEGAWA, S. 1971 Thickness of falling liquid film. *Tech. Rep. Kyushu Univ.* **44**, 299–304.